ME72 Engineering Design Laboratory
Final Team Design Report

Apex Cleanup: Summit, Mint, Bank

PharaoBots

Ana Jaramillo
Anya Mischel
Daniel Brito
Hannah Ramsperger
Lily Dong
Miina Anvelt
Sophia Andrews

Instructor: Prof. Michael Mello
Course: ME72 Engineering Design Laboratory
Terms: Fall–Winter
March 25, 2026

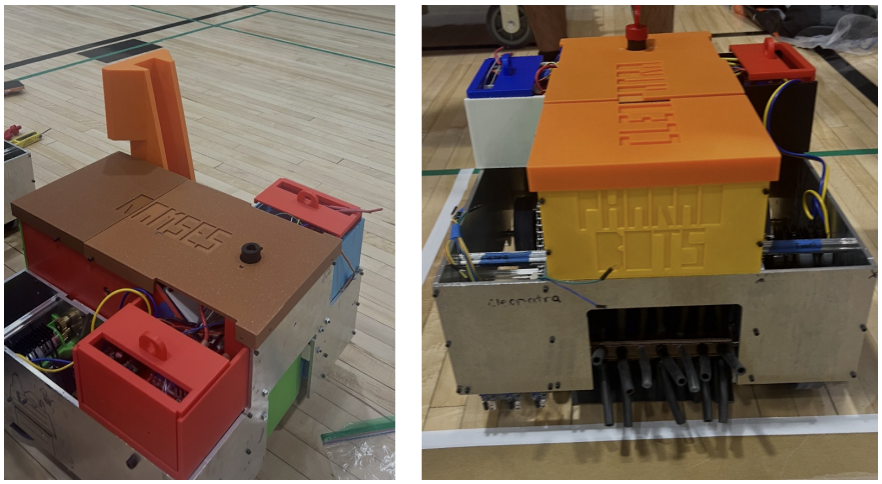

Final robot design used in the ME72 competition, Ramses (left) and Cleopatra (right).

Contents

1 Introduction and Competition Overview

Apex Cleanup is a multi-robot engineering competition in which teams design and operate up to two robots to collect, transport, and score game pieces within a structured competitive environment. The objective of the game is to accumulate the highest total score during a timed match by efficiently gathering radioactive pellet objects and depositing them at designated scoring locations while navigating a complex shared field and interacting with opposing teams.

Matches take place on a 40-ft by 40-ft field centered around a large pyramid structure with a steel surface and 37incline that serves as the primary high-value scoring location. Each match lasts 4 minutes and 30 seconds and consists of an initial 30-second autonomous period followed by a 4-minute teleoperated period. During the autonomous periods, robots operate without driver input to complete preprogrammed tasks such as pressing a beacon button for bonus points and follow a taped line using sensors to collect pellets. Afterward, robots transition to being driver-controlled and freely traverse the field to collect and score game pieces. A diagram of the arena is shown below.

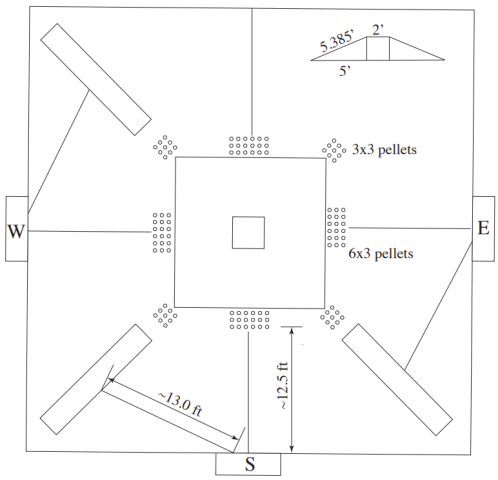

Figure 1: Field diagram of the arena.

The primary game objects for this competition are green pellets distributed throughout the field. Teams may deposit these pellets into slightly above ground-level depots (with an angle of incline much shallower than 37), or transport them to their associated Apex Summit location at the top of the central pyramid. Depositing green pellets into the depots generates gray pellets, which score points (with a significant tax) if they remain in the protected scoring zone beneath the depot by the end of the match. Alternatively, green pellets (or re-collected gray pellets) may be delivered to the summit to generate Energy Credits, which are high-value scoring objects released from the pyramid and by default transfer into team vaults for protected scoring. Additional major bonuses are awarded for successful pressing of the beacon (with a larger bonus for being first) and for robots that retrieve their own generated Energy Credits and redeposit them into their team's vault prior to reaching the vault naturally.

Scoring thus rewards multiple strategic approaches: strong autonomous operation and speed of line-following, large-quantity depositing at lower beacons, and successful summiting of the central pyramid to access the highest-value scoring option. Since combat between robots fighting for the same pellets and general fighting on the pyramid is allowed, ensuring that the robots have sufficient torque to resist pushing and a strongly enforced chassis and protected intake mechanism is vital.

The field layout and constraints from the rules document present significant engineering challenges. Due to the wide distribution of pellet clusters across the arena, rapid ground traversal and effective and an consistent intake mechanism are vital. Furthermore, the elevated pyramid introduces demanding climbing and stability requirements, as robots must ascend ramps, include small funnel openings for pellet depositing, and maintain a high enough clearance to crest the summit. Strategy-wise, teams must decide how to balance a heavy, low center-of-gravity robot design specialized for pushing and combat with a light-weight and high enough clearance for summiting robot design for fast driving towards pellets and quick acceleration. Additionally, since all teams deploy two robots simultaneously, the option to specialize each robot for particular tasks further complicates game strategy.

2 Game Strategy and System Architecture

In the early stages of the competition the intention was to have a pusher robot and a speed robot. By the end of the fall term we determined that both robots were going to end up being very similar. Additionally, we realized that we were no where close to being the fastest or strongest robots on the field. As such, the entirety of the mentality going into the winter term revolved around creating two similar robots that could each independently complete all tasks including intake, climbing, and depositing. This would ensure that if one of the robots was rendered inoperable during competition, the other robot's performance would not be directly impacted. While there were small differences in certain lengths between the two robots, these adjustments were made as slight improvements on the design from the first term, and were not meant to provide a significant difference between the two. Both robots had the same functional drivetrain design, electronics, and intake design. The biggest difference between the two robots was motivated by the autonomous section of the competition. While one robot would pick up pellets, the other had to hit a button located 16 inches off the ground. This meant that a vertical 3D printed arm was placed on top of our robot designated Ramses while our second robot, Cleopatra, had no extension. Additionally, Ramses utilized IR sensors to allow it to line follow, although backup hard code was implemented during the competition. Cleopatra used hard code from the onset to gather pellets.

Leading up to the actual competition, and following the slightly poor results of the mock, our expectations were set low. Our goals were simply to avoid robot contact as much as possible, especially against teams that seemed intent on playing aggressively, like MechE Wednesday: Afterparty, and The Clanks. This was especially true for combat on the pyramid, since testing showed that without a slow and careful descent, our robot was susceptible to flipping over. We also had no intention of risking a topple of our robot by having it go down the brachi in order to get a clean catch bonus. We planned on only depositing on the pyramid if it was clear. If this was not deemed safe, then our strategy

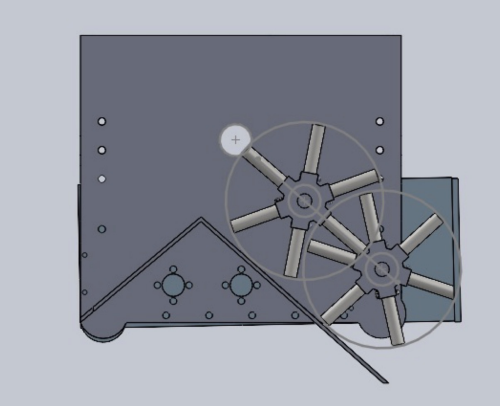

Figure 2: Inital intake arrangement

would be to use the depots. Our goals were also to assess the other robots during the actual competition and adapt accordingly. We also chose to only use two drivers to ensure that our driving would be as consistent as possible. The way our strategy evolved is detailed further in Section 10 Competition Performance.

3 Design Process

3.1 Concept Generation

An initial brainstorming session yielded a one-way intake-dumping system. The vision was always to including a collecting assembly at the very front of the robot, something to propel the pellets along the length of the robot, then a depositing mechanism at the very back. Some possibilities of the middle propelling including spindles and conveyor belts, essentially either something than was stationary and able to propel the pellets or something that was moving and taking the pellets with it. We decided on the former since conveyor belts will be difficult to implement and jamming would be a significant issue. A two way system where the pellets were both deposited and collected in a front opening through reversal of spindle rotation was also considered, but was then eliminated since it would greatly increase complications in driving in competition. Initially, the intake design had two spindle rods, however, since the first rods needed to be placed all the way in the front, a third row was necessary to put the pellets in the gathering area.

As for dumping, two approaches existed. One was to have propelling spindles all along the entire robot so pellets could be brushed out, the second was to have a ramp and only spindles along the first half (the ascending portion) of the ramp. The pellets will fall to a collecting pool on the descending portion of ramp. The second option was selected since it was simpler, and we wanted to minimize complexity of robot.

Lastly, the drivetrain was designed to have 4 motors, each powering a wheel either with bevel gears or chain and sprocket. The wheels needed to be large to ensure clearance at the base and top of pyramid. The drivetrain walls will need to stickout to protect the wheels somehow but not too much as to interfere with clearance.

Some other ideas were proposed including a drop-down arm with spindles for better

pellet collection in front of robot, side horizontal spindles to funnel pellets in for better intake, or vertical motor placement for higher weight distribution, but none were utilized due to complexity and difficulty of implementation.

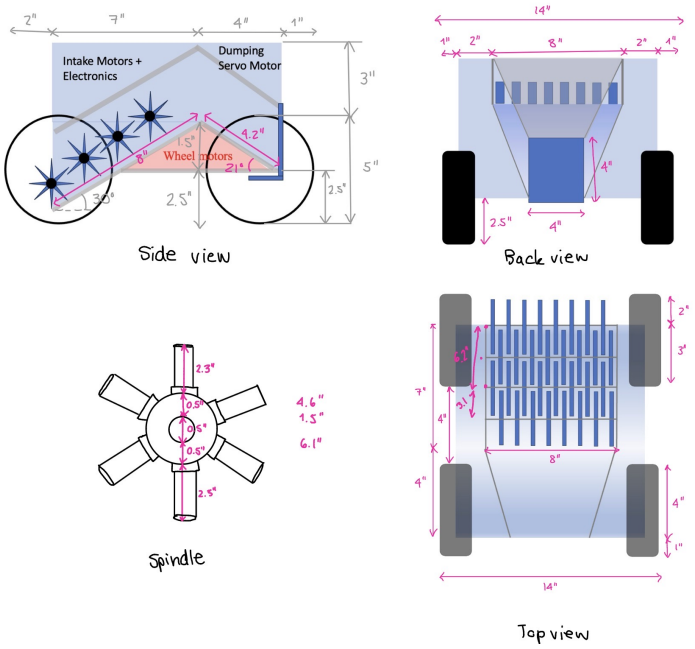

Figure 3: Design idea from PDR.

3.2 Engineering Analysis

3.2.1 Drivetrain Configuration

The torque requirements were calculated for the robot based on the 37-degree incline specified in the competition rules.

- Weight: 25 lbs = 111.20 N
- Rolling resistance coefficient: 0.04
- Force due to gravity on ramp: $F_g = W \sin(37°) = 111.20 \times 0.602 = 66.93$ N
- Rolling resistance force: $F_r = W \cos(37°) \times 0.04 = 111.20 \times 0.799 \times 0.04 = 3.55$ N
- Total force required: $F_{total} = 66.93 + 3.55 = 70.5$ N
- Using 5-inch wheels (0.0625 m radius):
- Total torque: $T_{total} = 70.5 \times 0.0625 = 4.40$ N·m
- Torque per wheel (4WD): $T_{wheel} = \frac{4.40}{4} \times 10.197 = 11.23$ kg·cm (1.10 N·m)

Futhermore, a 4-wheel drive configuration was selected over 2-wheel drive for reduced torque requirement per motor, redundancy in case of motor failure, and equal up/down ramp motion.

A gear tooth ratio of 26:20 was selected and the chain length has been calculated accordingly:

- Gear ratio $N = 1.3$
- Torque multiplier: 1.3
- Speed reduction: 0.77
- Chain length calculation: $L = \frac{2C}{P} + \frac{N+n}{2} + \frac{P((N-n)/2\pi)^2}{C}$
- Where $C = 2.5$ in, $P = 8$ mm, $N = 26$, $n = 20$
- Result: 39-54 chain links required

A motor performance analysis has been made as well with the selected motor: 42mm DC Planetary Gear Motor, 12V, 315 RPM

- Stall torque: 38 kg·cm (3.73 N·m)
- Rated torque: 20 kg·cm (1.96 N·m)
- No-load speed: 315 RPM
- Rated speed: 150 RPM
- Stall current: 12 A
- Rated current: 6 A

After applying the 1.3:1 gear ratio:

- Effective stall torque: $38.18 \times 1.3 = 49.63$ kg·cm
- Effective no-load speed: $315/1.3 = 242.3$ RPM
- Operating point for Climber: 1.10 N·m per motor
- Operating point for Runner: 0.79 N·m per motor

A stationary slipping analysis was conducted initally. The robot was analyzed for slippage when parked on a 37° incline:

$$\mu_S \times \frac{1 - X_c/X_w}{1 - \mu_S \times Y_c/X_w} \leq \tan(37^\circ)$$

Where:

- $\mu_S = 0.9$ (coefficient of static friction)
- $X_w = 10$ in (distance between wheel centerlines)
- $X_c = 4$ in (COM relative to back wheel centerline)
- $Y_c = 4$ in (COM height off ground)

Calculation yields $0.844 < 0.754$, confirming the robot will not slide on the incline.

Clearance calculations have also been made to inform about the drivetrain design:

$$\text{Breakover angle} = 2\arctan\left(\frac{5.54}{2.46}\right) = 132.19^\circ$$

Angle on top of incline: $53^\circ + 90^\circ = 143^\circ$ $132.19 < 143$, confirming adequate clearance.

Finally, approach and departure angle calculations were performed as well:

- Approach angle: 45° (conservative)
- Departure angle: 59°
- Ground clearance: 2.46 in at robot base

3.2.2 Intake Mechanism Analysis

For the intake mechanism the spindle torque requirements have been analyzed.

$$F = \mu mg\cos(45^\circ) + mg\sin(45^\circ)$$

For PLA pellets with density of 1300 kg/m^3:

- Pellet volume: $V = \pi r^2 h = \pi(0.625 \text{ in})^2(0.6 \text{ in}) = 0.736 \text{ in}^3$
- Pellet mass: $m = 0.01568$ kg
- Force per pellet: $F = 0.1523$ N
- With 3 pellets/row $\times$ 3 rows, torque required: $T = 0.0696$ N·m

3.2.3 Dumping Mechanism Analysis

For the dumping mechanism, the required ramp angle for the pellets to slide out without external force has been calculated:

For HDPE pellets on aluminum ($\mu_k = 0.2$):

$$\Theta = \arcsin(\mu_k) = 11.5^\circ$$

Due to the limited force of a servo, we added magnets to our design which should keep the back door from opening due to the weight of pellets. To hold 15 pellets (173 g):

$$F_{||} = mg\sin(\Theta) = 1.69 \text{ N}$$

Required magnetic flux density:

$$B = \sqrt{\frac{2\mu_0 F}{A}} = \sqrt{\frac{2(4\pi \times 10^{-7})(1.69)}{0.000322}} = 0.1149 \text{ T} = 1148.6 \text{ G}$$

Selected magnet: 2000 G rubber magnet (provides 5.12 N force)

We also analyzed the torque required for the motor to be able to open the door:

$$\tau = F \times r \times \sin(\alpha) = 0.1 \text{ m} \times 5.12 \text{ N} \times \sin(60^\circ) = 0.44 \text{ N·m}$$

Therefore, we selected MG995 Servo with 0.92 N·m.

3.3 Final System Architecture

Following the initial design discussions, the system architecture was organized into several distinct yet interconnected subsystems. This approach ensures that each subsystem can be developed independently while maintaining alignment with overall system engineering principles, facilitating parallel development across subteams. The architecture comprises the following key subsystems:

- Electronics
- Drivetrain
- Intake Mechanism
- Dumping Mechanism
- Upper Assembly Geometry
- Systems Integration

4 Mechanical Design

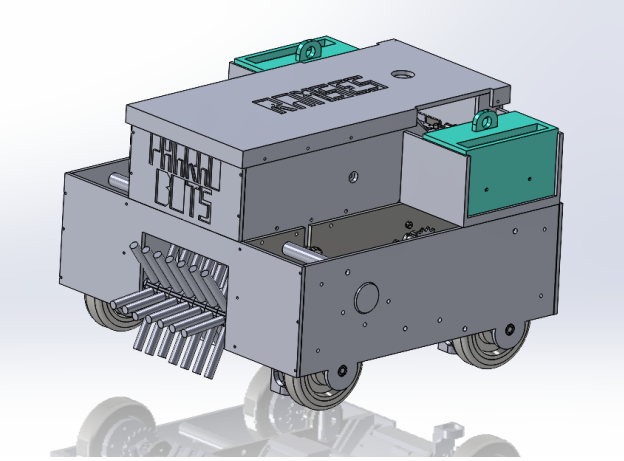

Figure 4: CAD model of the final robot design.

4.1 Drivetrain

Due to the plan of keeping two identical robots, we based the design of our robots' chassis on a simple box design due to its ease of machining, ability to replace parts without excessive material waste, and independence from other subsystems, including the intake and upper assemblies. Images of the drivetrain CAD are shown in the below figures.

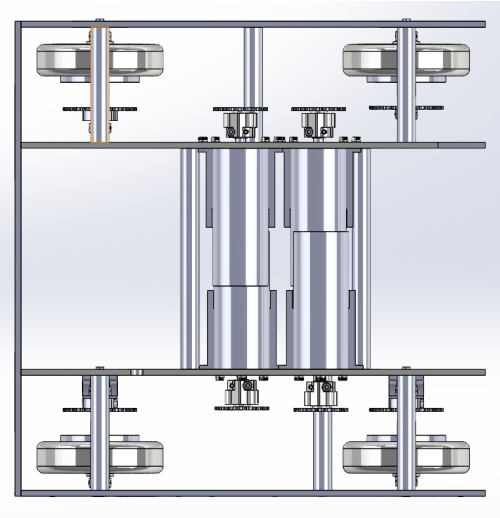

Figure 5: CAD model of drivetrain only, top view.

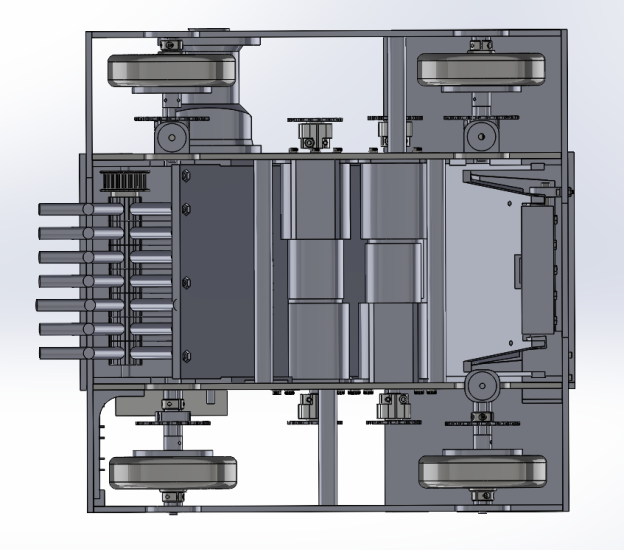

Figure 6: CAD model of assembly, bottom view.

We decided to use four-motor drive for both robots due to concerns over having sufficient torque to climb the steep incline of the pyramid. We chose 12 V, 315 RPM, 20 kg-cm torque integrated gearmotors from RobotShop with a gear ratio of 1/13 [1] for all four driving motors on both robots to match the calculated torque needed to stay on the pyramid without

slipping. We used chains and sprockets with a 1:1 gear ratio which connected each driving motor to its associated shaft. For the wheels, we decided to use sushi wheels with a durometer of 80 from the machine shop due to their balance between grip and durability.

The main drivetrain structure consisted of four parallel rectangular walls with semicircle additions on the bottom of each wall for the bearings which held the main driving shafts. This was chosen so that the robot could make the needed clearance for the robot to crest the top of the pyramid. A front and back plate held the entire assembly together using 4-40 screws. The front and back plates also protected the shafts from collisions and ensured that no other robot would come in contact with the wheels, chains, or any part of the shafts during combat. All four drivetrain walls were made from aluminum to keep the weight of the robot low while still maintaining high strength and durability.

The inner drivetrain walls contained mounts for the driving motors and attached to the upper assembly, which allowed the separation of the intake and drivetrain subsystems to keep them independent. We 3D printed semicircle mounts which also screwed into the drivetrain walls to further support the weight of the motors.

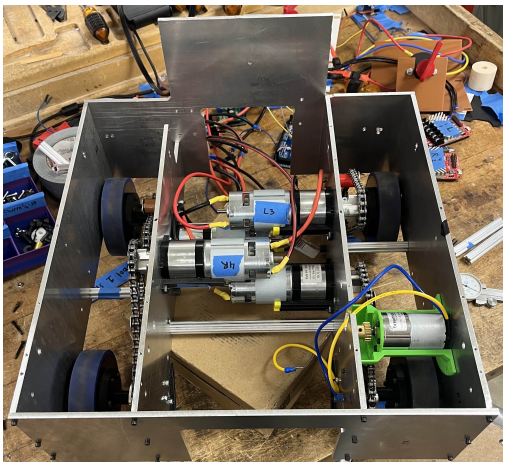

Figure 7: Machined drivetrain without upper assembly or intake subassemblies.

Between the inner and outer drivetrain walls, we included the shafts with the wheels and tension rods, aligned with flanged bearings on both walls and constrained axially through spacers between the sprocket and wheel hubs and the bearings. We elected for aluminum D-shafts to lower the moment of inertia of the rods and due to the shop's availability of aluminum stock. Due to constraints in manufacturing time and availability of large-diameter aluminum stock under the constraints of our budget, we elected to 3D print our wheel hubs and press fit them onto our shafts with set screws to further fasten the wheel hubs to the shaft. We also machined tension rods with a 3D printed outside part which tightened the chains and prevented the chains from skipping or falling off of the sprockets.

To further brace the main drivetrain walls from impact, which we expected a lot of during the competition, we installed 3 aluminum churros between each side of the inner and outer drivetrain walls and 2 churros between the inner drivetrain walls. Since we were significantly limited by the available stock of aluminum churros, we made the decision to decrease the distance between the inner and outer drivetrain walls for Cleopatra compared to that of

Ramses. The dimensions for the front and back plate were adjusted accordingly.

4.2 Upper Assembly

The goal of the upper assembly was to serve as the base structure for the intake and dumping mechanisms as well as the electronics while remaining independent from the drivetrain. This separation allowed the two systems to be integrated only during the final stage of assembly. Additionally, the design needed to accommodate the chassis configuration, which included four motors stacked vertically.

This motor arrangement was the primary geometric constraint, as it only allowed the intake mechanism to be mounted on an incline. To address this, an intake ramp with the lowest possible angle was designed and connected to a rear gathering ramp, which was also inclined. The resulting intake ramp angle was 47°, and a cutout was required to accommodate one motor that protruded into the ramp space. The structure is shown in Figure 8. Because the ramp needed to reach the floor for effective intake, but the available clearance did not allow a rigid material to extend that far downward, a rubber piece was attached to the end of the ramp. This made the final inch of the ramp flexible, allowing it to reach the floor while maintaining the necessary clearance. The length of the front ramp extending upward has been determined by the placement of the three intake rods, which have been placed 3.9 inches apart, and 2.5 inches above the front ramp.

The design of the back ramp was fully constraint by the front ramp design and length of the drivetrain. Since the depot opening on the pyramid was 4 inches, a controlled release of the pellets would only be possible if pellets exit the robot in a 4 inch wide opening. However, since the back ramp was wider than 4 inches, the pellets needed to guided to the 4 in wide opening. A funnel has been designed as shown in Figure [**?**], which consisted of a wall of each side of the back ramp which was placed diagonally, and secured with screws into the bottom thickness though the ramp, and a slot in the ramp.

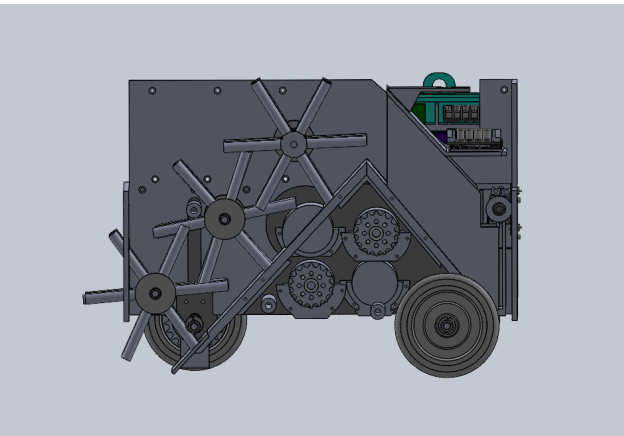

Figure 8: CAD of inside view showing ramp structure and spindle arrangement.

The upper assembly side walls held the ramps together. The walls included slots for the ramp, as well as several slots and cutouts for screw heads sticking out from the drivetrain assembly. A front and a back plate secured the the upper assembly from lateral movement

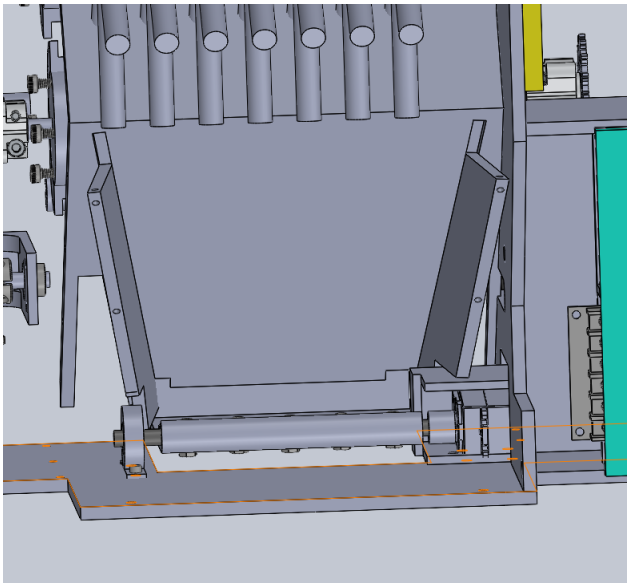

Figure 9: CAD zoomed into back of robot showing funnel structure and dumping door being placed inside of the robot for protection.

as well as the top plate, which has been designed as a lid. The side walls had the electronics storage integrated in the back of the robot.

4.3 Intake Mechanism

The scoring mechanism consisted of two parts: The intake collected the pellets and the dumping mechanism deposited them to score.

The intake mechanism was intended to utilize spindles instead of rubber wheels from very early on due to the size and rigidity of the pellets. We also considered 3D-printing them with TPU, but decided to opt for surgical tubing, a softer and bouncier material, instead. As soon as the dimension and material for the spindle was chosen, the intake hubs were designed. They were gear-shaped hexagons with six holes for spindle attachment. A M6 screw goes in each hole and were screwed in until they reach the intake shaft, mimicking the function of setscrews while also regulating uniform spindle stick-out. Two types of intake hubs were designed, full-sized with a thickness of 0.75" and half size with 0.55" thickness to ensure offset of spindles so they do not come in contact with each other during motion and create unnecessary friction. Three rows of spindles were utilized, each row comprised of a 0.25" diameter steel D-shaft and 6-7 intake hubs with 6 spindles on each one. The middle row was powered by the intake motor through two 1:1 gear ratio gears; it connects to the first and last row with two timing belts. The first and last row each had one timing belt pulley while the middle had two. Pulleys and gears were both fastened with setscrews.

Figure 10: Intake Assembly of Both Robots before Final Assembly

4.4 Dumping Mechanism

The dumping mechanism was responsible for depositing the pellets onto the pyramid or depot. The pellets were collected along the inclined back of the upper assembly and funneled into a 4-inch-wide outlet. At this point, a door prevented them from falling out before reaching the designated deposit opening. To prevent the weight of the pellets from accidentally opening the door, a magnet was used to secure the door to the underside of the back ramp.The door was mounted on an aluminum rod connected to a servo on one end and to a hinged bearing on the other. An MG995 servo was secured to the inside of the back plate using a custom holder, alongside the hinge. The dumping assembly is shown in Figure 11. The holder, hinge, shaft connector, and door were all 3D-printed components. The entire dumping mechanism was mounted to the back plate and positioned approximately 1 inch inward from the rear of the robot, allowing the back plate to act as a protective barrier for the mechanism.

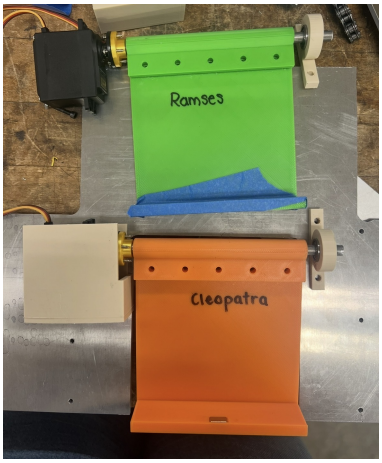

Figure 11: Assembled Dumping Mechanisms for Both Robots Before Full Robot Assembly.

4.5 Magnets

Due to height of the robot as well as the weight, the drivetrain itself was not able to climb. Therefore, magnets were added to the drivetrain. To account for the clearance, the magnet mounts were been placed right next to wheels on the outside of the inner drivetrain walls, with four magnets per robot. The magnet mounts were designed so that the magnetic force pulling the magnets on the mounts to the steel incline pulled directly down rather than torquing the mounts. This way, the mounts could be 3D printed to last multiple rounds. Additionally, the clearance between the ground and the magnets needed to be very small for the force to be large enough to effectively hold the robot on the incline without slipping. This further justified the use of the 3D printed mounts, so various clearances could be tested and replaced easily.

4.6 System Integration

The drivetrain and the upper assembly have been put together by sliding the upper assembly in between the inner drivetrain walls. Due to the nature of the design after putting the two subsystems together, they were in the right place and only needed to be secured with 3 4-40 screws on each side screwing through the upper part of the inner drivetrain walls into middle-height placed holes in the upper assembly walls.

The electronics have been integrated through designed electronics storage as well as cutouts for wires. The cutouts for the drivetrain motor wires have been placed on the sides of the back ramp, and cutouts in the back of the side walls on top allowed wires to go from electronics storage to the desired place. To make use of the unused space above the back ramp, a electronics deck has been designed, held by the funnel walls, to put the Arduino on it, which ideally is placed right below the switch. The beacon presser was places above the wheels with a cover plate and a height of 16 inches to be able to press the beacon. A cutout in the cover has been for the IR sensor wires to connected from the front wheel placement to the Arduino in the back on top of the funnel. Electronics storage covers have been designed to be easily put on an removed after driving the robot to disconnect Lipo batteries and battery packs fast. The safety switch was placed on top for fast accessibility.

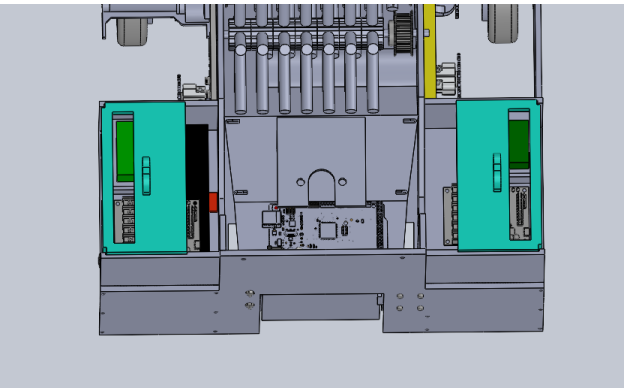

Figure 12: CAD of electronics management.

5 Electronics and Control Systems

5.1 Electronic components

We detail the full list of electronic components used in Table 1, wires excluded. We note that the components used were equally divided between both robots with the exception of all IR Sensors and the Breadboard which were only used on Ramses, our button presser robot. We note that that for both robots there was a designated Left and Right Roboclaw. The directionality of each roboclaw corresponds to the motors on one side of the robot that the roboclaw controls, and not the relative position of the roboclaw in the electronics box of the bot. For example, in the final design, the left roboclaw controlling the left two motors was positioned on the right side of the robot.

Component	Quantity
2x30A Roboclaw	4
Arduino Mega 2560	2
Flysky FS-i6X Controller	2
FS-iA6B receiver	2
32V, 70A Fuse	2
Diode 100V	2
12V Battery Disconnect	2
2k, 1/4 W Resistor	4
Pololu TReX Dual Motor Controller DMC01	2
HW201 Infrared (IR) Sensor Module	3
Turnigy Nano-tech 2200 mAh 4S 45–50C LiPo	2
5 x 1.5V AA Battery Pack	2
Main Wheel 42mm DC Planetary Gear Motors	8
DC Gearmotor 121 RPM	2
Solderless Breadboard	1
10M Ring Connectors	12
MG995 Servo	2

Table 1: Complete list of electronics components across both robots

5.2 Power connections

A diagram of power connections can be seen in Figure 13. The two power sources for all electronics in both Cleopatra and Ramses are a **Turnigy Nano-tech 2200 mAh 4S 45–50C LiPo** and a **5x1.5V, AA Battery Pack**. The battery pack was used solely to power the **Arduino Mega 2560**. Note that this battery pack was swapped for a portable charger due to inconsistencies with the battery pack cabling during both the mock and the final competition. The rest of the electronics were powered by the LiPo battery.

The LiPo Battery's power cables leads immediately to a **70A Fuse**. This is a slow blow fuse designed to protect against any large surges in current. The fuse was chosen based off the peak current expected from the system x 1.3 to provide an additional tolerance for safety.

From the fuse the power goes into a **12V disconnect switch** which allowed us to control power to the rest of the system. Across the switch we ran a **100V diode** to provide a path back to the battery when the switch is opened and the motors are ran. This is primarily a safety measure. Across the switch are also two **2k, 1/4 W pre-charge resistors** to avoid high inrush currents and arcing.

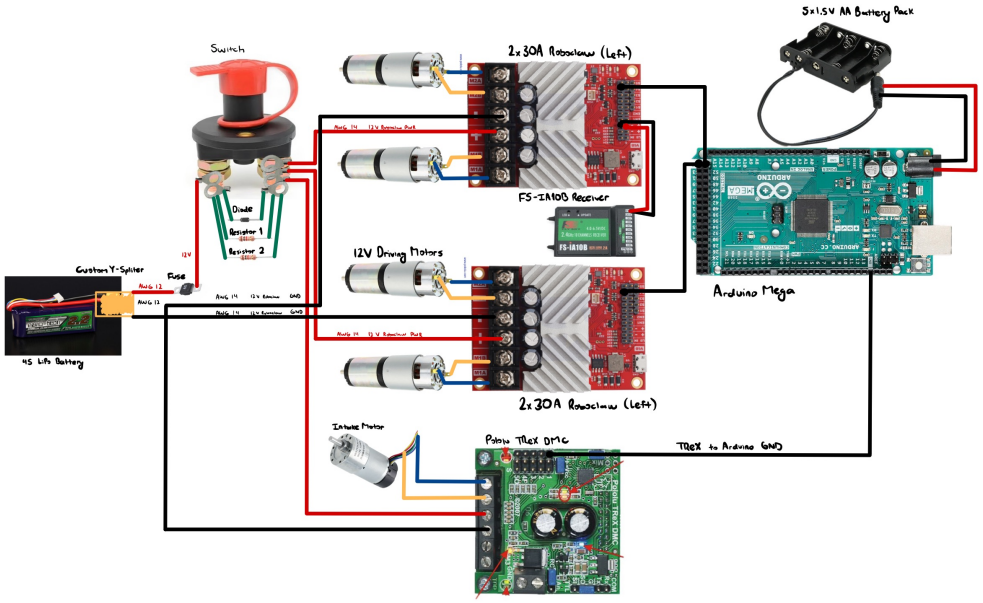

Figure 13: General power wiring for both robots

On the other side of the switch the power wire is split three ways. Two of the power wires goes to two **2x30A Roboclaws** each. The third power wire goes to a **Pololu TReX Dual Motor Controller DMC01**. The ground wires are split three ways immediately after the battery and each go to the Roboclaws and Trex. All wires used are either 12 AWG and 14 AWG. This also includes driver motor wires. The use of each gauge varies depended on the robot but it was determined at minium 14 AWG would be required to handle current loads. The left Roboclaw also powers the **FS-iA6B receiver**. That same Roboclaw also powers the three IR sensors on Ramses. For these connections as well as the intake motor, jumper wires were used. Ground wire connections are also made between the Arduino and Roboclaws, a Roboclaw and receiver, and the TReX and Arduino.

5.3 Logic architecture

The center of all logic used for driving both directly and autonomously was the **Arduino Mega 2560**. The general logic wiring for Cleopatra and Ramses is shown in Figure 14 and 15 respectively. Both follow the same structure with the only difference being that Ramses has a **Breadboard** and 3 **IR Sensors**. The **FS-iA6B receiver** is powered by the Left Roboclaw with ground and power wires connecting each.

The receiver communicates all inputs from the controller to the Arduino via iBUS. This connection is achieved by connecting the iBUS TX on the receiver to RX2 on the Arduino.

This signal is decoded inside of code written in the Arduino IDE. The receiver contains one other direct connection being the connection to the **MG995 Servo** backdoor motor, which is made directly and without an Arduino. A signal wire, power wire, and ground wire is connected to the corresponding CH10 on the receiver.

The arduino uses serial communication to transmit signals to the roboclaws. S1 and S2 on the right Roboclaw are connected to TX1 (Pin 18) and RX1 (Pin 19) on the Arduino respectively. S1 and S2 on the left Roboclaw are connected to TX3 (Pin 14) and RX3 (Pin 15) on the Arduino. PWM signals were used between the Arduino and TReX. S1 on the TReX was connected to PWM Pin 5.

For Ramses, three IR sensors are connected to the Arduino. The left IR sensor signal wire was connected to PWM Pin 3 on the Arduino, the center one was connected to Pin 4, and the right IR sensor was connected to PWM Pin 5.

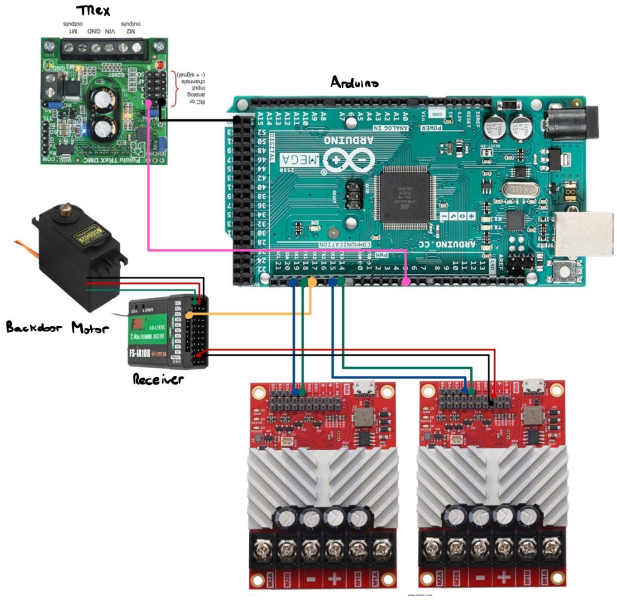

Figure 14: Logic wiring for Cleopatra

5.4 Driving Modes and Logic

The **FlySky FS-i6X controller** was configured to use 10 channels according to Figure 16. Channels 1-4 are assigned to the joysticks. Channels 5-8 are assigned to switches. Channels 9 and 10 are assigned to knobs. We then coded three modes that the robot could use: normal drive mode, climbing mode, and autonomous mode. Here we detail normal drive mode and climbing mode which remained the exact same across both Cleopatra and Ramses.

In both normal drive mode and climbing mode, CH5 activates autonomous mode. Both CH7 and CH9 were used to activate the intake motors at different points however during the competition the intake motor was assigned to CH7 to allow for faster on and off control. CH7 is a switch that has three possible positions. These were configured such that the first switch position turned the intake off, the second position caused the intake to run at 60% speed, and that the third position caused to the intake to run at 100% speed. CH8 was

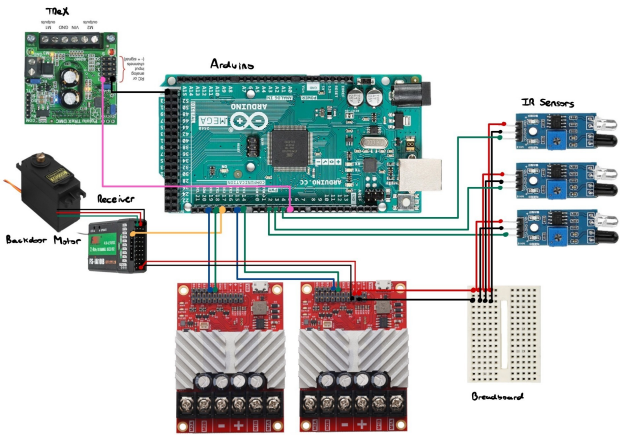

Figure 15: Logic wiring for Ramses

assigned to swittch between normal drive mode and climbing mode, with normal drive mode being the default on startup. CH10 was used to control the backdoor servo motor.

When normal drive mode is on (CH8 off), CH2 will allow for forward and backward acceleration, CH1 allowed for left and right turning, and CH3 was used as a throttle limiter, meaning its position determined the maximum possible speeds of driving and turning. For example, if the CH3 is positioned halfway up (50%) and CH2 is maxed out forward, then the robot will only go at half of the possible maximum speed. We use differential turning. The positions of CH2 and CH1 are first scaled by the position of the throttle limited (CH3). The command to the left motors is then given as CH2 + CH1 and the command to the right motors is given as CH2 - CH1. Depending on the value of CH1, this corresponds to a left or right turn.

When climbing mode is on (CH8 on), driving is inverted relative to normal drive mode. This means that a forward movement is now made relative to the back of the robot since our robots most consistently climbed up the pyramid backwards. The following assumes that the back of the robot is assumed to be the new front. In climbing mode, CH3 now sets a constant velocity. CH2 and CH1 still allow for forward & backward movement and turning respectively. However they are no longer throttle limited by CH3. Turning (CH1) is still limited by a constant value of 0.6, set in the code. Climbing mode allows for our robot to position itself at the base of the pyramid, align itself, and climb up at constant speed with CH1 allowing for small adjustments in turning.

5.5 Autonomous Code

As previously mentioned CH5 allows for autonomous mode to be switched on and off. Due to the limited amount of working IR sensors at our disposal and the geometry layout of the arena, it was decided in the final weeks that only one robot, Ramses would employ IR senors for line following. This would be our button presser. The other robot, Cleopatra, would use calibrated hard-code. During testing, inconsistencies with the IR sensor calibration led us to create a back up hard code for Ramses that could be uploaded during competition in the event of IR sensor failure. This proved to be a prudent decision as, during competition, the

Figure 16: Controller channel configuration

IR sensors broke forcing us to fall back on the hard code.

The IR Sensors were designed to be placed 1" apart from each other, as our lower distance limit was set by the width of the white and black tape and our upper distance limit was set by the drivetrain area in which we were going to place the IR sensors. IR sensors were strategically placed in front of our one the wheels so as not to interfere with the climbing clearance and the intake ramp. This meant that the robot would not be centered on the line and the code was calibrated accordingly. Three IR sensors were used to detect the line. The center IR sensor was used to detect the white center-line and the other two sensors were used to help guide the robot in case it deviated off the line. The IR sensors were then calibrated to provide the correct output depending on the color of the tape. The code was written such that depending on the sensor reading, the robot would either stay in the line or deviate from the line. For the code to successfully work, driving speeds and turning speeds were also calibrated and set based on each motor's actual output. Later, a memory was added to the code to help alleviate noise and any wrong signals read by the sensors. The memory, which was calibrated, averaged the last set of data points to make sure that each reading was consistent over a specified period of time.

The hard code relied on the same commands that were defined for the IR sensor code. These commands were executed based on calculated times. For example, **Ramses's hard code** simply commanded the robot to travel forward at roughly 60% of the maximum speed for 6.34 seconds. This time was chosen based off of testing inside the machine shop. The speed was chosen to be fast enough to beat other robots without being so fast that the initial acceleration would cause the robot to end up misaligned. For **Cleopatra's hard code** which was the main and only autonomous mode used for pellet collection, the code followed operations based on table 2 where fwd refers to forward movement. A slow forward and medium forward command were also implemented that would run the motors at 18% and 36% the maximum speed respectively. The slow forward command was used whenever the robot was picking up pellets. This ensured that the robot could pick up as many pellets as possible without running over them which would impact alignment. The medium forward command was used between the first batch of pellets and the second batch to ensure that the robot could reach both sets of pellets before the 30 second autonomous period ended. We note that the entirety of the Cleopatra autonomous code takes 25 seconds to run giving

5 seconds before the end of the autonomous period. The intake motor was also switched on and off at different points to ensure that it was not being run the whole time. This was done to avoid intake motor over heating, which was an issue with the first intake motor that was used during the mock competition.

Time (s)	5.55	1.20	8.25	2.20	0.80	1.60	4.40	1.00
Driving Command	fwd	left	slow fwd	med fwd	med fwd	right	slow fwd	stop
Intake Status	off	on	on	off	on	on	on	on

Table 2: Cleopatra autonomous code. Time indicates for how long a given driving command is given.

6 Fabrication and Construction

6.1 Material Selection

The final two robots are structurally made from aluminum with supporting pieces made from PLA 3D printed material. The main material selected was aluminum due to its properties as a lightweight and durable material. Furthermore, one of the main design emphasis for the robot was ensuring the protection of all internal components whether it was the intake mechanism, dumping door, or the drivetrain itself. Due to this, while initial plans for the robot considered having the walls end prior to the end of the wheel diameter, this was redesigned to extend the walls in front of the front wheels and behind the back wheels, allowing for additional front and back plates which previously were not included in initial designs.

During manufacturing, the idea was considered of having HDPE or acrylic made up the structure of the front plate. However, this was later disregarded due to the impact benefits of including an aluminum front plate. The selected aluminum was a sheet of 0.2" nominal thickness which tended to be 1.998" thickness when constructing the robot. This choice of thickness was somewhat coincidental as initially the design plan was to use 0.25" thickness for the two outer walls of the robot however after considering budgeting and material constraints this was reduced to 0.2" thickness. In the end, the 0.2" thickness was likely advantageous to the overall design by having less of an added weight than the 0.25" thickness walls would have been.

For internal components, most structural elements were made from 3D printed PLA materials such as housing all electrical components, magnet holders, the rotating part of the tension rod, the ramp, the interior intake walls and all hubs on the intake. The main two reasons for this choice of material were that it is (1) lightweight and (2) easy to form into a desired shape from a CAD model. For elements such as the interior walls, while an initial idea was making these from HDPE, the walls themselves consist of a very specific angled slot, three high tolerance holes for bearing, as well as multiple other miscellaneous holes for robot integration. Maintaining the level of accuracy required would only have been possible

with a waterjet or a laser cutter but as HDPE melts in the laser cutter when tested on test pieces and the smaller water jet would not be able to fit the dimensions, the walls were 3D printed.

Other elements, such as the electronics holder or hubs, were made with PLA to ensure that they did not contribute significantly to increasing the weight of the robots and changing its center of gravity. The magnet holders were chosen to be made with 3D printed material, since it was determined that the advantage of having them interchangeable to change their distance to the ramp outweighed the benefits of machining them. Thus, based on the above choices, the material selected for the structural enclosure was aluminum and the material chosen for other highly unusually shaped non-structural elements was PLA 3D printed material.

6.2 Machining Operations

The first version of the robot was completed using the waterjet by maximizing the dimensions of the waterjet and pausing the cut prior to any undesired cuts being made. After the design was changed to be longer and protect all of the drivetrain components in the second term, the main forms of structural outline machining were completed with the TRAK milling machine, any circular components with the lathe machining, rough cuts with a bandsaw, and any additional hole elements with the drill-press. Since, unfortunately, the larger waterjet in the machine shop used for this project was broken and not serviced within the duration of the project, all larger metal structural parts were completed using CNC programming on the conventional milling machine. While this was a steep learning curve from the content covered in general machine shop procedures for ME13, members of the team scheduled meeting sessions with Trent to discuss how to set up the mill for CNC automated cutting based on a user-defined program. After testing some basic CNC machining on a test part, all eight main structural walls of the drivetrain wall were cut using this method.

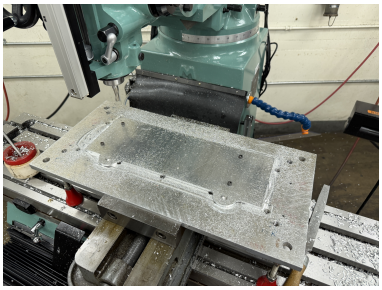

Figure 17: Mill setup to drill holes into drivetrain walls.

One of the challenges faced with choosing to go with this machining process was the time intensiveness required of it. From creating a CAD to model all of the outer wall dimensions relative to a second base plate, setting up the vice clamp ends on the mill to be backwards, to setting up the program fully in the milling machine, this effort involved verification on multiple levels prior to the first cut even being made. While the milling allowed for precise cuts to be made and holes to be drilled at exact CAD defined locations, the process would have been much faster had a Waterjet been used. Since there were no slots or particularly

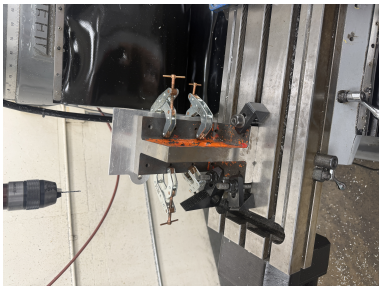

Figure 18: Mill setup to drill holes into thickness of drivetrain walls.

unique geometries that required a mill, it was not being utilized for its main purposes beyond cutting edges and drilling holes. Despite these various challenges and disadvantages to using the mill, the advantage of having the whole outer wall as a continuous piece still largely outweighed the disadvantages. If the whole drivetrain walls had not been cut as a continuous piece, the other options for joining it would have been welding or 180-degree brackets. In the case of the brackets, they wouldn't have been as structurally strong and learning to weld would have been time-intensive as well. Thus, using the mill with a programmed path based on CAD allowed for all the walls to meet the specifications of the design and maintain structural integrity.

The lathe was also used extensively when making structural components such as the churros and the tension rods for the robots. When creating the first version of the drivetrain for the robot last term, the team was not as concerned about the tolerances on the churro lengths. However, after testing in the first ever demo last term, it was noted that the robot struggled since the slightly different churro lengths resulted in some sections of the drivetrain being more constrained than others. This led to slanted walls both inwards and outwards, which would not work with the intake design that was planned to slot between two vertical inner drivetrain walls. Due to this, Cleopatra was made using the old churros after using the lathe to cut them down all to the same size. The length of the churros for the side ended up being 3.54 in for Cleopatra while the ideal size that was expected from the CAD was kept for Ramses. The churros were all cut to size on the lathe as well as taped to allow for a $\frac{1}{4}$-28 screw to fit for the churro. All tension rods were also created using the lathe and they were cut down to the diameter dimension desired using a cutting tool before switching to the part tool to cut down the rods to a specific size. The material of the churros was aluminum and the tension rods were made from a 0.75 in outer diameter scrap material, also likely aluminum. When completing the machining with the lathe it was noticed that occasionally the lathe, especially lathe 1, would be off-center from its alignment and this made the machining process harder as the tools wore down.

Overall the machining process ended up relying heavily on the lathe and conventional mill, while all other miscellaneous machining was completed with the drill press or hand drill as needed.

6.3 3D Printing

The 3D printing process was used for all miscellaneous parts that required specific geometries and would have been time consuming or not possible to machine in any other way. As mentioned in the machining process section, the main parts 3D printed were the electronics holder, the intake walls, the ramp, the funnel for dumping, as well as the magnet mounts. For the electronics holder specifically, it was initially designed in term one to have an overhang over the sides that allowed it to sit on top of the robot and slot above the drivetrain walls. For the second term, with added electronics components to allow for the intake motor and the servo motor to also be connected, such as the arduino Mega board, the electronics box design expanded as well. The final version extended above the drivetrain walls at the back of the robot leaving space for the arduino to be placed in the center section while roboclaws were off to the side. This design not only allowed for improved wire management but also for ease of access in the case that any wire became loose. This design, specific to the dimensions of each of the electronics components and having a stacked layer to allow for two layers of electronics, was only possible through 3D printing. Similarly, in order to meet the specific requirements for the ramp slot angle, and match it on both sides, as well as meet the tolerances of all the intake rods bearing shafts, the intake walls were chosen to be made using 3D printed material.

The other main structural component that was made using the 3D printer were the magnet mounts. These were made with at least four walls of infill when printing to ensure their strong structural integrity and were redesigned on multiple occasions based on the various tests completed. For example, after one of the demonstrations in the second term, it appeared as though the added weight of the intake and the electronics holders was limiting our ability to climb fully. To fix this issue, a new magnet mount was designed which had the capacity to hold two magnets rather than one. While this design iteration did not end up being used, other changes to the design, such as making it have a smaller amount of material surrounding the magnet did stay. By having this component be 3D printed, it allowed for the flexibility to switch small mechanical elements, such as the distance from the bottom of the mount to the ground, or how it was attached, without requiring a long re-machining process everytime. This was significant as it was noted that these mounts were interchanged on many occasions throughout the term when making clearances smaller or redesigning them to be more accessible.

Another significant part that was 3D printed were the wheel hubs. As it was difficult to find any commercial parts that would attach the wheels onto a $\frac{1}{4}$ radius shaft, the wheel hubs were chosen to be 3D printed. The main reason this method of manufacturing was chosen was to reduce the machining required to create the wheel hubs as the wheel choice was also changed over time. However, the disadvantage to using 3D printing for this specific purpose was that it wore down significantly faster than expected over longer term testing such as during the competition. Due to this, after the round-robin matches the team realized the wheel hubs had been fatigued to the point where the hubs were rotating on their own relative to the shaft. While the team had replacement parts to fix this, for future designs it likely would have been more effective to use a more fixed machined part for this component. Furthermore, this issue indicated the limitations of using 3D printing for main structural drivetrain components as it wears fast with an applied load.

The intake hubs were also created using 3D printing material which involved specific tolerances for a press-fit of the $\frac{1}{4}$' radius shaft and to ensure that the plastic screws for the surgical tubing were able to fit. In early iterations of the design the hubs often came out printed with a center radius hole that was outside of the desired tolerance. Due to this, each 3D printer machine where this part was printed was kept track of to understand its tolerances and print to within the tolerances. Along with this subsystem, it was noted that often the plastic screws used to attach the surgical tubing became worn out after using them two or three times. Due to this, the amount of times these screws were removed and reinserted into the hubs was limited when possible to avoid the plastic material wear.

Thus, while 3D printing was effective for creating non-structural components that were not loaded over time and had to be interchanged based on testing, it was less effective for the drivetrain components that experienced significant forces over time.

6.4 Waterjet Fabrication

The waterjet was not used as significantly for the fabrication of the final robots as other machines such as the mill and the lathe. However, the waterjet was used for test parts and verification of tolerances. For example, when determining which reamer to use for the bearing holes, different hole sizes were created using the waterjet and then reamed with different reamer sizes. The final hole size for the bearing holes ended up being 0.495 in for any waterjet part and the drill bit that was one size smaller than the $\frac{1}{2}$ in drill bit. The reamer based on the waterjet test part was 0.498 in. The waterjet was also planned to be used for the front support pieces that attach to the front plate. However, the waterjet was broken in the lab area the day prior to the competition so this part did not end up getting cut out. Thus, the waterjet supported the fabrication by allowing the fast creation of test pieces and components based on the CAD design.

6.5 Assembly Challenges

While the modular design that was selected for the robot allowed for ease of testing subsystems and made it simple to redesign the subsystems, assembly was one of the weaknesses of the design. As the design did not consist of a fully standardized screw size, or standardized unit system of screws between metric vs customary, assembly per robot involved 4-40 screws to attach the front and back plates, metric screws to attach the motors, $\frac{1}{4}$-28 screws, $\frac{1}{4}$-20 screws, as well as other 4-40 screws for upper assembly and motor mount integration. In terms of fabrication, it was also difficult to gain access to the drivetrain walls once the robots were fully assembled. While this was advantageous to the final robot, it was often challenging to access the inner drivetrain wall specifically to make updates such as adding another hole for a new component that would need to be incorporated. With respect to the machining timeline this was also a challenge as the drivetrain walls were completed early in the process to allow for assembly but also were the components that, when required to be fixed or updated, led to the robot requiring disassembly often. Thus, for future improvements, the assembly could have been considered as a greater area of concern when designing the full modular design to ensure ease of access.

7 Testing and Experimental Evaluation

7.1 Subsystem Testing

7.1.1 Drivetrain Speed Testing

Frequent tests of the drivetrain's functionality were performed throughout the entire duration of the project. The first major benchmark was to have one robot fully able to drive, navigate a set of cones, perform a speed test, and climb the pyramid. For this demo, we set the goal of only having a drivetrain (without the upper assembly or intake subassemblies) in order to focus all of our attention on drivetrain while spending more time carefully designing the intake mechanism. For this test, we machined the four parallel drivetrain walls with the first selection of our wheels. In this test, we confirmed the ability of our robot to drive and turn, but struggled with climbing. Leading up to this test, we found multiple errors which we were able to fix, such as adding tension rods to prevent chain skipping. The first demo revealed that the tires of our first set of wheels separated from our hubs. To fix this, we installed magnets and replaced our wheels. *Figures 19* and *20* show tests of the robot climbing and navigating around cones, respectively. Further tests throughout the second term, including the mock competition, allowed for repeated testing of accelerating and turning, and revealed additional issues with our drivetrain, such as incorrectly sized spacers, ineffective magnet mount designs, and loosening tension rods, all of which we corrected for the final competition.

Figure 19: Drivetrain prototype for first drivetrain mobility demo

7.1.2 Pellet Handling Efficiency

Intake testing was split into several phases. All testing dimensions were initially consistent with theoretical analysis but adjusted according to testing results.

Phase 1 was the testing of geometric fitment and dimensional tolerance, specifically for timing belt length and hole sizing on intake hubs. Hub holes went through several iterations

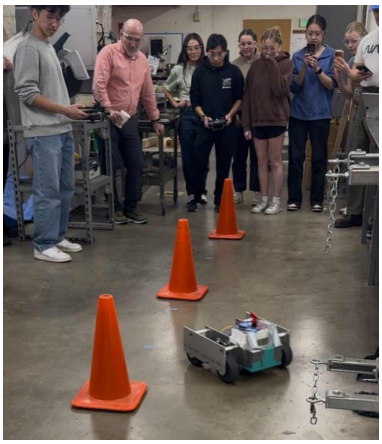

Figure 20: Navigation test for mobility demo with drivetrain prototype

of fitment testing both for M6 screws and shaft since a press-fit effect was desired. The 3 rows were designed to be parallel to the intake ramp and 3.9" apart. Holes were prototyped on wood and belt tension was tested after pulleys were installed.

Phase 2 was spindle length testing at the first intake demo. Spindle length was tested flush against table and cut at 2". This proved too short after mounting on drive train. It could successfully intake ECs but were to short for pellet collection. First row spindle length was then increased to 2.5" while second and third row remained at 2".

Phase 3 focused on optimizing collection efficiency after intake was proven to work successfully. The increase in length caused decreased rigidity of spindles, resulting in decreased efficiency in picking up pellets. Side gaps at the intake ramp also caused pellets to get stuck instead of being swept up. Modifications were added to magnet mount to solve ramp gap issue and 3 PVC spindles were added to each of the 3 middle hubs of the first intake row. This seemed to increase collection efficiency.

7.1.3 Climbing Mechanism Evaluation and Brachi Testing

After trying to climb without magnet during mobility demo, magnet mounts have been added to the drivetrain. Since a low clearance is necessary for the magnets to be effective, but uneven terrain does not allow a too low clearance, iterative testing with different clearances has been made. By adding the whole upper assembly, additional weight caused the clearance to decrease again which has been shown during testing. Lower clearance has been tested right before competition day, and the mount broke. Therefore, an ideal clearance has been determined which is able to make the weight of the robot climb while still having enough tolerance. Furthermore, initially testing showed that we need to climb up with the back in the front.

We also tested the ability of going down the Brachi. The first tests have been made with a leash to catch the robot in case it is tipping. The testing showed that the robot needs to go down with the front first. Also, adding weight at the bottom of the drivetrain lowers the center of gravity and this made the robot go down the brachi successfully.

7.1.4 Dumping Mechanism Testing

The dumping mechanism has been tested isolated without intake during winter term by connecting the servo and moving the door. Once the robot was assembled for Handling Demo I, the dumping mechanism has been tested in an temporary setup for the first time, showing that impact can open the servo door. The final dumping assembly was ready for Handling Demo II, and showed that it works effectively if the robot is placed right above the depot. However, this testing series showed that the shaft connector is an important part and should be screwed instead of pressfitted with a 3D print. Furthermore, if the robot experiences an impact, the dumping door opens slightly causing pellets to fall out. Therefore, magnets have been added, and this newly added feature has been tested to to choose magnets that are strong enough to hold the door but not too strong so that the servo can still overcome the magnetic force.

7.2 Field Testing

Field testing unveiled several issues concerning collection reliability and consistency. At the mock competition, pellet collection was highly variable with the robot sometimes collecting a full load of pellets but mostly struggling to collect even a few. The intake motor was overheating to dangerously high temperatures that almost melted the 3D-printed motor mount as well as stalling around 2 minutes into testing. Heat sinks were tied to the motor to temporarily dissipate the heat but results weren't significant. Vibrations of the robot also caused meshing issues between the two intake gears, often resulting in substantial wear on the gears and the intake stopping altogether. Troubleshooting yielded valuable information and exposed a couple of issues. Firstly, the intake motor was not outputting an adequate amount of torque. What seemed to be enough in benchtop testing proved unfit for the real field as pellets got stuck on the speed bump of the ramp and rigid PVC spindles hit the front plate. This created a significant amount of load on the motor previously unaccounted for, resulting in stalling and possibly over heating. Secondly, the angle of the intake ramp speed bump was too sharp for the pellets to go over but just large enough that they nestled perfectly against it, halting the flow of collection. Lastly, the magnet mounts helped a lot in preventing pellets from getting stuck, but some were still sneaking past and getting driven over by the wheels.

A couple of solutions were generated for the issues mentioned above. A new intake motor will be purchased. An ideal one similar in size but rated to output 5 times as much torque was chosen and a new motor mount that attaches to both drivetrain walls was made to minimize vibrational effects. The speed bump on the ramp was cut off, leaving one drivetrain motor exposed but at a much less angle than previously. Some PVC tubing was removed to minimize contact with the front plate, leaving 1-2 on each of the middle 3 hubs. They were also cut around 0.2" shorter. The intake hubs were reprinted and system was reassembled to eliminate loosening of the press fit.

8 Design Evolution

The overall design concept of the robot was established prior to the preliminary design review, with the configuration shown in the figure serving as the foundation for subsequent design evolution. A CAD model was developed for the critical design review to verify the mechanical feasibility of the proposed structure. By the time of the CDR, the drivetrain CAD had reached a high level of detail, enabling prototyping. The upper assembly CAD continued to evolve throughout the fall term, adapting to both drivetrain modifications and changes in competition rules. Most design updates were implemented following key milestones, such as the mobility and handling demonstrations, where areas for improvement became clearly apparent.

During the fall term, the primary focus was on developing a reliable drivetrain. To validate the motor arrangement, chain lengths, and clearances prior to machining in aluminum, a drivetrain prototype was fabricated from DFT wood, as shown in Figure [**?**]. This prototyping phase revealed the need for tension rods. After confirming the viability of the design, the full drivetrain was machined from aluminum and prepared for the mobility demonstration at the end of the term. The mobility demo indicated that climbing required the addition of magnets and revealed a flaw in the initially purchased wheels. As a result, magnets were incorporated and new wheels were assembled, after which the climbing demonstration was repeated.

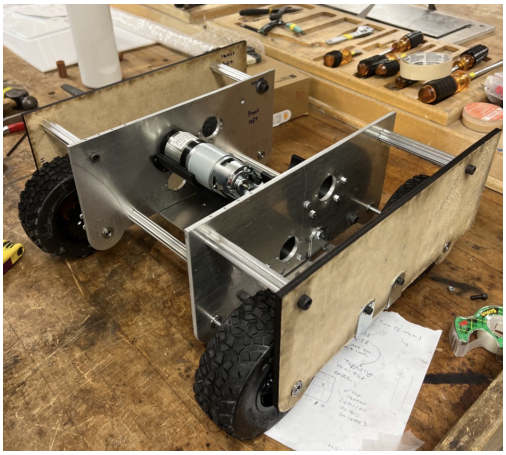

Figure 21: First drivetrain prototype.

With the preliminary and critical design reviews in mind, the upper assembly, including the intake and dumping mechanisms, was also developed. The dumping mechanism was prototyped using a simple setup consisting of a rod connecting the servo to the door. The intake, however, was not prototyped during the fall term. As a result, the upper assembly primarily evolved within the CAD environment throughout the term. Nevertheless, feedback from the PDR and CDR confirmed that the design was reasonable.

Entering the winter term, the drivetrain had been validated to reliably climb and complete a slalom course. However, several improvements were still necessary. To better protect the drivetrain during combat, the side walls were extended beyond the wheel length, preventing direct exposure of critical components. Additional churros were incorporated to increase

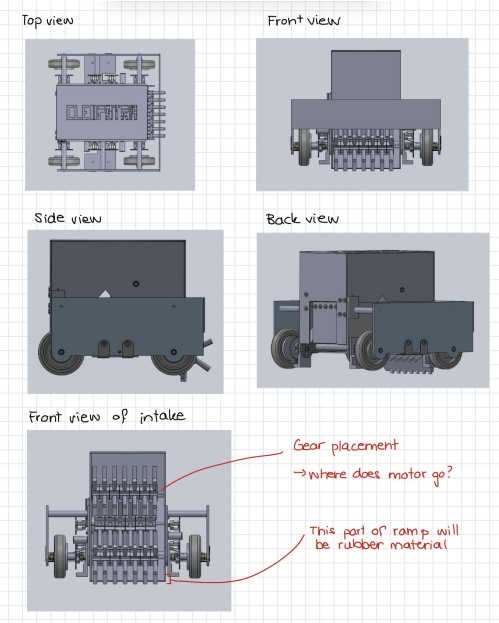

Figure 22: State of CAD at the end of fall term.

structural stability. Despite these modifications, the overall functionality of the drivetrain has remained unchanged since the mobility demonstration.

During the winter term, the focus shifted to the upper assembly, including the intake and dumping mechanisms. Since the high-level design decisions had already been made in the fall, prototyping began early in the term to ensure functional subsystems. The dumping mechanism had been designed in great detail in CAD and translated well into the physical implementation. The ramp and side walls were also prototyped. Initial system integration, conducted in preparation for Handling Demo I, revealed issues with the approach of sliding the upper assembly into the drivetrain, due to protruding screw heads and intake rods. This led to the addition of slots and cutouts to prevent similar issues in subsequent prototypes.

During Handling Demo I, concerns about the intake spindles being too short were con-

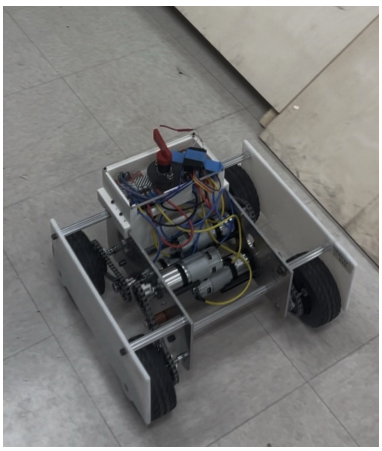

Figure 23: Drivetrain with temporary electronics storage during mobility demo.

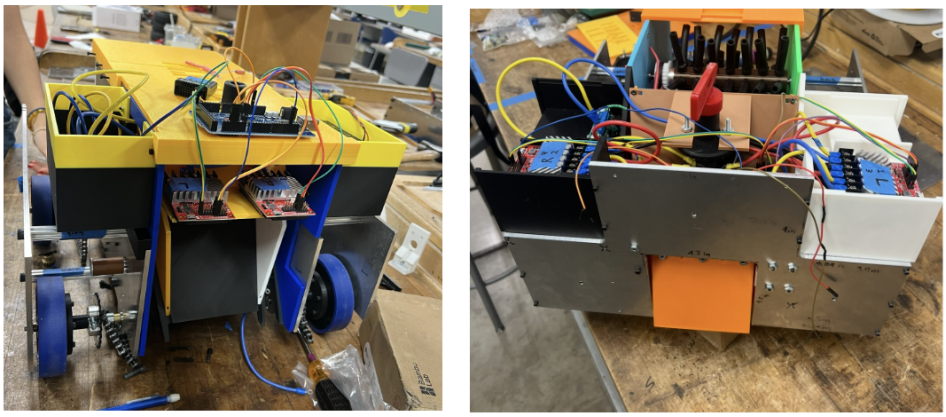

Before handling demo II

After handling demo II

Figure 24: Wire management evolution

firmed. Since the back plate had not yet been machined, the dumping mechanism was tested using an improvised rear assembly, which nonetheless demonstrated that the concept was viable. Following this demo, efforts focused on machining the back plate and fabricating new intake rods with longer spindles.

For Handling Demo II, both drivetrains and back plates were machined, allowing full assembly of the dumping mechanism. The intake was reassembled with longer spindles. While gear meshing was temporarily resolved using tape, this exposed a more fundamental issue: excessive vibration caused by 3D printed bearing and motor mounts made the meshing unreliable. Additionally, intermittent intake failures due to disconnected wires highlighted the need for improved electronics management. As a result, electronics storage was integrated into the rear portion of the side walls rather than mounted externally, and the safety switch was relocated to the electronics deck to enable quicker access and repairs.

During mock competition testing, the intake motor was observed to overheat. Heat sinks were added as a temporary solution, but it became clear that a higher-performance motor would ultimately be required. At the same time, complete loss of gear meshing prompted the design of a critical aluminum support component to stabilize the middle intake rod and eliminate vibration. This proved highly effective and resolved the issue. Additional improvements included adding magnets to prevent the dumping door from opening under impact and replacing an unreliable press-fit shaft connector with a screwed connector. A beacon presser was also designed and positioned above the wheel to enable line following.

Further issues identified during mock competition included intake motor stalling due to pellets becoming lodged near the speed bump cover. This was addressed by redesigning the front ramp with a cutout to provide more clearance. The rubber ramp, which had been bending backward, was shortened, and a guiding rubber element was added in front of the wheels to prevent pellets from being run over and instead direct them into the intake.

Final testing before competition focused on resolving magnet mount clearance issues that affected climbing performance. Additionally, after the robot flipped shortly before competition, aluminum reinforcements were added to the 3D-printed upper assembly side walls. These final adjustments, along with improved wire management, resulted in a highly

reliable robot. Continuous iteration after each demo and testing session led to significant improvements across all subsystems, culminating in strong performance on competition day.

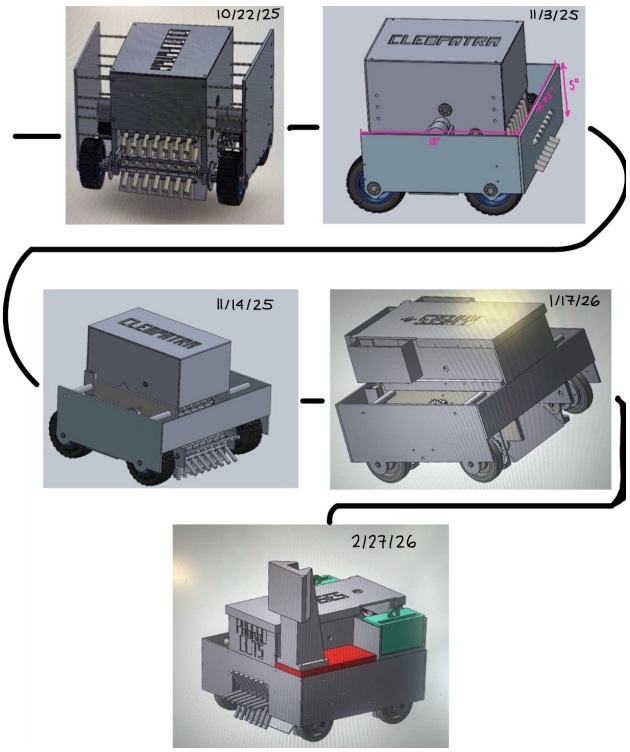

Figure 25: Design Evolution

9 Competition Performance

Match outcomes
The PharaoBots competed in 5 qualification matches and 2 elimination matches. The team achieved 5 wins, finishing 2nd overall in the qualification ranking and finishing 1st place in the whole competition. Performance improved over the course of the competition as adjustements were made to drive control and game strategy. The strongest match occured during the final round, where the robots achieved its highest score of 25 points.

Scoring Statistics
Across all recorded matches, the robot achieved scores between 10 and 25 points, with an average score of approximately 17 points per match. The final match produced the highest score of 25 points, indicating improved efficiency in completing scoring tasks compared to earlier matches. Table 9.1 summarizes the scores achieved by the PharaoBots robot during the competition.
Reliability Observations
Both robots demonstrated generally reliable intake and electrical performance throughout the competition. However, several reliability issues were observed in the drivetrain system.

Match	Score
1	10
3	20
4	8
6	17
9	13
E2	22
Final	25

Table 3: PharaoBots competition scores across all recorded matches.

During Match 4, Ramses' drivetrain chain slipped out of the gears, which reduced robot mobility and scoring efficiency. In addition, the autonomous line-following routine failed during Match 4 because one of the IR sensors broke while the robot was climbing during the previous match.

A more significant issue was identified with Cleopatra after Match 9, when the robot was no longer able to climb. Upon inspection, the team determined that the 3D-printed wheel hubs were slipping on the motor shafts because the press-fit was insufficient. Backup wheel hubs were available, and the team requested a timeout before the elimination round in order to replace three of the four wheel hubs.

After this repair, Cleopatra was able to successfully climb the depots during the final two matches, although Ramses remained the only robot to successfully climb the large pyramid. However, Cleopatra's inability to climb the larger pyramid forced the team to adjust the game strategy by using Cleopatra robot to focus on depositing pellets in the depot while Ramses prioritized climbing. This adjustment unexpectedly improved overall scoring efficiency and contributed to the team's strongest performance in the final matches.

Comparison to Expected Performance

Prior to the competition, the robot was designed to achieve consistent scoring primarily through depot and grey pellet banking, as well as autonomous beacon activation. However, the team did not expect to achieve particularly high scores, as the robot particularly designed for constant battling. The team expected significant contact between robots near the pyramid, which could potentially push the robot off the pyramid and lead to mechanical damage during matches.

In practice, the level of robot-to-robot contact was significantly lower than anticipated, which allowed the robot to operate more consistently than expected. Additionally, it wasn't among the team's strategy to go down the brachi to intercept and collect ECs, and it was assummed that other teams would this approach to optimize their scoring. However, during the competition, no team used the brachi, which resulted in overall scoring being lower than anticipated.

As a result, the robot's performance relative to other teams was stronger than initially expected.

10 Budget

Component	Quantity	Cost ($)
Main Wheel 42mm DC Planetary Gear Motors	8	351.60
Chain (8mm Pitch Steel)	2	23.98
Chain Linking Pack	1	2.99
Drive Wheels	4	69.99
Stealth / Sushi Wheel Replacement	4	0.00
Aluminum Stock	1	70.00
PLA Gold Filament	1	22.99
HDPE Sheet	1	31.72
12V Battery Disconnect	2	20.58
32V Fuse	2	5.22
Flanged Ball Bearings	3 Packs	28.87
Latex Surgical Tubing	3	47.42
Clear Plastic M6 Screws	7 Packs	46.83
8mm Pitch Sprocket 16 Tooth	8	18.32
8mm Pitch Sprocket 22 Tooth	8	22.32
1309 Series Sonic Hub	8	63.92
1310 Series Hyper Hub	8	63.92
Shaft Collars	1 Pack	16.25
Diode 100V	2	0.62
Churros	3	28.50
Locknuts 4-40	1 Pack	9.11
Ring Terminal Connectors	12	9.12
Metal Gear	4	71.96
XL Timing Belt Pulley	7	86.24
Greartisan DC Gear Motor	2	29.98
XL Timing Belt	4	28.64
Neoprene Rubber Sheet	1	6.68
Neodymium Magnets	4	15.80
Zip Ties	1 Pack	3.99
Air Duster	1 Pack	3.95
DC Gearmotor 121 RPM	2	64.99
Total		1266.70

Table 4: Summary of project expenses.

11 Engineering Standards and Safety

11.1 Safety

Proper measures were taken to ensure safety when wiring, prototyping, and utilizing electrical components. LiPos were handled with measures in accordance with the LiPo Battery Tutorial Spring 2024 provided by the MCE department. LiPos were stored in safety bags when not in use, while prototyping, and while charging. LiPo monitors were always connected during any battery usage. Voltage drops and current were calculated to ensure that the appropriate wire gauges were used. This included the use of 12 AWG wire for the connections between the battery and switch and 14 AWG for all connections after the switch. Appropriately sized ring connectors were used at the switch and Roboclaw to ensure clean wire disconnections. All connections were soldered, crimped, and covered with heat shrink and/or electrical tape where applicable. Wire terminal crimp connectors were also used to connect the motor and power wires to the TReX.

A diode, switch, resistors, and fuse were all chosen on the recommendation of the BasicMicro Motion Control user manual, and were used during all prototyping and tests. The specific values of the aforementioned components, including voltage and current, calculations, and a factor of safety was applied to all components depending on recommendations from Trent and the Roboclaw manual. All electrical components, including the Roboclaws and battery, were secured to an electronics box with Velcro to eliminate movement which could lead to damage. For the final competition, all jumper wire connections were hot glued together to prevent wires from disconnecting.

11.2 Standards

The following engineering standards were taken into consideration when designing, fabricating, and testing. Dimensioning and tolerancing practices were guided by ASME Y14.5 to ensure that machined parts could be manufactured reliably. Standard fasteners were selected following ASME B18 specifications to improve compatibility and ease of replacement. Material choices, including aluminum for structural components, were informed by ASTM material standards to ensure predictable mechanical properties and machinability. Electrical wiring practices were influenced by ASTM F1883 guidelines to promote safe routing and reliable connections. For wiring gauges we used the **American Wiring Gauge standards** as set by **ASTM B258**. The Flysky FS-i6 controller utilized in our project has a radio frequency range of 2.408 - 2.475GHz which falls under the **FCC Part 15 for unlicensed low-power communications**.

12 Lessons Learned and Future Improvements

12.1 Strengths

Overall, choosing two have two identical robots (minus the inevitable adjustments to the space between in the inner and outer drivetrain walls) was a good decision which greatly

reduced complexity of design and machining and allowed our robots to be competitive during the competition, since both robots could (at least initially) perform all tasks.

Reflecting on our design process, we found that testing parts independently was very effective when we needed to resolve design issues and working as separate subteams on the project. This was particularly helpful for fixing specific parts, as an issue with one part would only affect that part's subassembly, rather than the entire robot.

As for the drivetrain, extending the four parallel walls past the wheels allowed for the parts required for driving, intake, and dumping to be completely protected throughout the entire competition. The inclusion of the front and back plates out of aluminum not only protected these assemblies, but also improved the general chassis strength by reinforcing all side walls with one solid base. The addition of churros was also very effective at bracing the walls and keeping a resilient structure during collisions. Furthermore, the inclusion of tension rods was extremely effective at preventing chains from skipping or falling off, and mounting the tension rods on both the inner and outer drivetrain walls ensured that the screws rarely came loose despite repeated wear. The addition of magnets was also critical for climbing and worked effectively with 3D printed mounts by the end of the project, since they could be easily reprinted and tested to optimize the clearance from the ground and design of the mount. Magnets helped add an effective normal force to the pyramid when climbing without adding weight to the robot and decreasing its speed.

As for the intake subassembly, the choice of using surgical tubing for the intake was effective and our final motor choice was specced well to avoid stalling during the competition. Furthermore, having modular parts reduced the reliance of the entire intake on one printed part, though it came at the cost of rather difficult assembly and disassembly. Furthermore, the addition of more rigid tubing enhanced the grip and allowed the pellets to be more forcefully pushed up the intake ramp. Having three rows of this tubing was also critical for getting the pellets up the intake ramp, since the distance the pellets had to go up was rather large for an intake motor of the speed we selected. The addition of the rubber gathering ramp and side gathering rubber pieces also aided in increasing the overall efficiency of the intake, despite having a narrow intake width compared to the width of the robot. The speed of the intake was also chosen well to strike a balance between being fast enough to pick up pellets and slow enough to not accidentally push or reject them. The intake motor being supported by both drivetrain walls was also very effective in preventing the intake motor from rotating accidentally and kept the gears meshing.

As for the upper assembly, the entire assembly worked well together, and 3D printing the walls came with the advantage of being able to easily change locations of holes and add complex geometries. The addition of side boxes attached to the upper walls on the back of the upper assembly greatly improved the wire management and allowed for an easily accessible electronics configuration. Furthermore, the connections between the upper assembly and drivetrain in multiple places, as well as to the back wall, allowed the upper assembly to fit well within the entire robot assembly rigidly. The dumping mechanism was very effective and reliable throughout the entire competition, and the angle of the ramps was chosen strategically to allow maximum volume for the storage of pellets while still being able to easily slide out into the top deposit holes on the pyramid. The later addition of aluminum supports to the upper assembly walls also reinforced their stability and prevented cracking when our robots rolled down the pyramid

Finally, the electronics proved to be reliable and easily testable, which was vital for testing and ultimately provided an important point advantage during the autonomous section. Our robots managed to win the beacon advantage in almost every round due to the consistency of the line-following, and gained a major advantage in the collection of the front and corner groups of pellets for the other robot during the autonomous section. The switch with a large handle allowed for easy testing of the electronics and its implementation allowed for a safe way to instantly shut on or off the robot, such as instances in which the arduino lost power and the robot went rogue. Furthermore, the use of iBUS significantly reduced the number of wires needed between the receiver and arduino.

12.2 Weaknesses

While many of the strengths contributed to success in the competition, both of our robots exhibited many weaknesses, especially throughout earlier phases of the design processes, which decreased performance.

As for the drivetrain, the tall robot design created a particularly high center of gravity, which caused the robot to sometimes tip and roll down the pyramid when the robot drove over pellets when driving down the pyramid. This was originally caused by the use of four drive motors rather than two, since fitting four motors in line with the motors we selected was not possible and ultimately created the constraint that some of the motors had to be install vertically higher than the others. Additionally, the original wheels chosen were not high quality, and the outer tire of the wheels rotated with respect to the inner hub which caused the robot to completely lose traction when attempting to climb up the pyramid. The second set of wheels were much better, but eventually the hub we used for the wheels came loose due to being 3D printed and we ran out of time to make the hubs out of aluminum or pin them to the shaft. Additionally, since the turning for the robot was about one of the back wheels, this wheel tore and got very worn down during the competition. Additionally, due to budget, we mostly used spacers to prevent the shafts from sliding out of the bearings on the drivetrain walls. However, it was very easy to lose the spacers and we did not have proper documentation or labeling on the lengths of the spacers, which made it very difficult to track them and we frequently had to replace them. As for the magnet mounts, earlier designs had the magnet placed slightly off center rather than being directly below the wall, which caused the magnet mounts to warp slightly due to the torque of the magnetic force on the mount, which lowered the clearance unevenly and resulted in drifting when driving up the pyramid.

As for the intake, the width of the intake was generally quite small relative to the width of the robot which decreased the overall efficiency of the robot. The pulleys and belt were placed on the inside of the inner drivetrain walls, which caused a rather large loss to the width of the intake. This gap also caused the pellets to get stuck when going up the ramp under the pulleys. Furthermore, having 3D printed hubs on the intake shafts frequently resulted in the hubs wearing down and the press fit would eventually come loose. The biggest weakness in the earlier version of the intake subassembly was the intake motor selected, however. The motor was much too low in torque and would overheat and stall very easily, making it very difficult to intake during the mock competition. The use of better specced motors during the final competition greatly improved the performance of the intake. Another weakness

with the final version of the intake subassembly was that one of the spacers on the middle section was cut slightly too long, which pushed apart the upper assembly walls a bit and had a butterfly effect on the full assembly, resulting in difficulties fitting the drivetrain walls together.

In general, having many different, complex parts meant that it was very difficult to assemble and disassemble the entire robot, which made testing very difficult. While the original intention was to have the upper assembly slide into the drivetrain and operate independently from the drivetrain, this did not end up working as anticipated since some parts had to go through both the upper assembly walls and the drivetrain walls and inherently prevented this idea from working as hoped. This ultimately made assembly and disassembly extremely challenging and likely more difficult than it would have been to design and machine the inner drivetrain walls to include parts for the upper assembly. Furthermore, due to this complexity, we did not have enough time to make the upper assembly walls out of HDPE, which we had hoped to use due to its resistance to shattering compared to PLA. Instead, we had to rely on the 3D printed upper assembly walls, which broke easily when the robot unexpectedly rolled down the pyramid during certain rounds of the competition.

As for the electronics, the use of PWM and Serial communication caused signal issues with the TReX that would cause the motor to stutter. To fix this, we would have to use a better motor controller for the intake and/or implement serial communication between the arduino and intake motor driver. Furthermore, the use of AA battery packs meant that the Arduino power was inconsistent, especially during testing. If the voltage dropped too low, the Arduino would stop being able to send signal to everything else. A small Lipo to power the arduino would have remedied this issue. Finally, the IR sensors were not protected enough at the front of the robot and ultimately broke off, causing the robot to be hard coded for the last few rounds of the competition. Better casing with the 3D printed mount likely could have prevented this.

References

[1] E-S Motor. 42mm dc planetary gear motor, 12v, 315 rpm. `https://www.robotshop.com/products/e-s-motor-42mm-dc-planetary-gear-motor-12v-315-rpm`, 2026.

[2] International Organization for Standardization. (1989). General tolerances Part 1: Tolerances for linear and angular features without individual tolerance indications. ISO 2768-1:1989.

[3] International Organization for Standardization. (2021). Geometrical product specifications (GPS) — Geometrical tolerancing — General geometrical specifications and general size specifications. ISO 22081:2021.

[4] ASME. (2019). Fasteners for use in structural applications. ASME B18.2.6-2019.

[5] ASME. (2019). Dimensioning and tolerancing. ASME Y14.5-2018 (R2024).

[6] Federal Communications Commission. (1989). Part 15—Radio frequency devices. 54 FR 17714, Apr. 25, 1989.

[7] ASTM International. (2013). Standard practice for selection of wire and cable size in AWG or metric units. ASTM F1883-03 (2013).

[8] ASTM International. (2018). Standard specification for standard nominal diameters and cross-sectional areas of AWG sizes of solid round wires used as electrical conductors. ASTM B258-18.